Calcium phosphate nanoparticles as nuclei for the preparation of colloidal calcium phytate

Kathirvel Ganesan and Matthias Epple*

Received (in Montpellier, France) 6th March 2008, Accepted 29th April 2008
First published as an Advance Article on the web 23rd June 2008
DOI: 10.1039/b803903h

Colloidal calcium phytate was prepared by anion-exchange of phosphate by phytate, starting from calcium phosphate nanoparticles. Scanning electron microscopy (SEM) showed spherical nanoparticles of narrow size distribution, in good agreement with dynamic light scattering (DLS) results, whose diameter could be adjusted between about 40 to 250 nm depending on the employed synthesis conditions. The particle surface is covered by phytate anions as indicated by the strongly negative zeta potential of −40 to −50 mV. The preparation of a stable colloid was only possible within a narrow range of the ratio of calcium to phytate. Infrared spectroscopy, X-ray diffraction and elemental analysis showed that the particles consisted of X-ray amorphous calcium phytate. The colloidal dispersions were stable for about two weeks before precipitation occurred.

Introduction

Phytic acid, *myo*-inositol-1,2,3,4,5,6-hexakis(phosphate) is a member of the isomer family of 1,2,3,4,5,6-hexakis(phosphate) cyclohexane with a six-fold substitution of phosphate. It is characterized by a high density of phosphate groups which are able to interact with a calcium phosphate surface. It is an abundant biomolecule in humans, animals and plants and therefore of high biocompatibility.[1,2] Like other organic phosphates, it has a cariostatic effect that was ascribed to its ability to inhibit the dissolution of tooth enamel by strong adsorption of phytate to the calcium phosphate surface of enamel.[1] Thereby, it is able to prevent the formation of cavities.[3–6] There are reports on the prevention of kidney stone formation, of protection against diabetes mellitus, caries, atherosclerosis and coronary heart disease as well as against a variety of cancers by dietary phytate.[7] Its value as food component was extensively reviewed by Harland and Morris[1] and Greiner *et al.*[7] Calcium phytate is an effective absorbent for heavy metals such as lead.[8,9]

NMR spectroscopy has shown that phytic acid adopts two conformations in an aqueous solution that switch by a change of the pH value (Fig. 1).[10–13] Due to its six phosphate groups, it has a strong chelating effect to bind multivalent cations which can lead to an undesired depletion of metals such as Zn^{2+}, $Fe^{2+/3+}$, Ca^{2+}, Mg^{2+}, Mn^{2+} and Cu^{2+} in the body.[1,7] In the presence of calcium ions, it forms insoluble calcium phytate. An *in situ* precipitation of calcium phytate together with radioactive cations leads to a dispersion which is used for scintigraphy and also commercially available as a kit.[14] However, the particle size in this dispersion lies between 100 and 300 nm, and the stability of the dispersion is only about 6 h at room temperature.[14] For instance, Higashi *et al.* have prepared Sn/Ca/^{99m}Tc phytate microparticles[15] which can be used for scintigraphy in the liver and the spleen.[16] Imam and Killingsworth have studied various colloidal dispersions for ^{99m}Tc for scintigraphy and concluded that the continuous growth of calcium phytate particle size is problematic for scintigraphic organ mapping which may sometimes be performed on the next day.[14] Al-Janabi has prepared ^{113m}In-doped calcium phytate colloids for liver scintigraphy.[17]

Nanoparticles of calcium phosphate occur in living nature as mineral in bone and teeth.[18,19] They are also found in animal and human blood where they are stabilized by suitable proteins such as fetuin ("calciprotein particles") and probably act as a calcium reservoir and as precursors for biomineralization.[20,21] This demonstrates the biological importance of dispersed calcium phosphate nanoparticles. Phosphate-substituted molecules appear to be especially effective in stabilizing calcium phosphate nanoparticles.[22–24] It was also possible to stabilize amorphous calcium carbonate (ACC) in the form of hollow microparticles by the presence of phytic acid.[25]

Here we present a method where synthetically prepared calcium phosphate nanoparticles were reacted with sodium phytate, leading to an anion exchange in the surface and

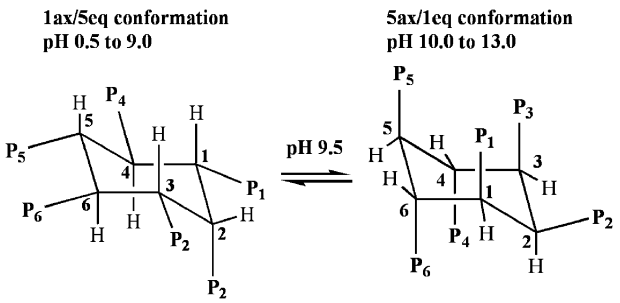

Fig. 1 The two conformations of phytic acid in water, depending on the pH: 5ax/1eq and 1ax/5eq; P = $-OPO_3H_2$, $-OPO_3H^-$ or $-OPO_3^{2-}$.

Institute of Inorganic Chemistry and Center for Nanointegration Duisburg-Essen (CeNIDE), University of Duisburg-Essen, Universitaetsstrasse 5-7, 45117 Essen, Germany. E-mail: matthias.epple@uni-due.de

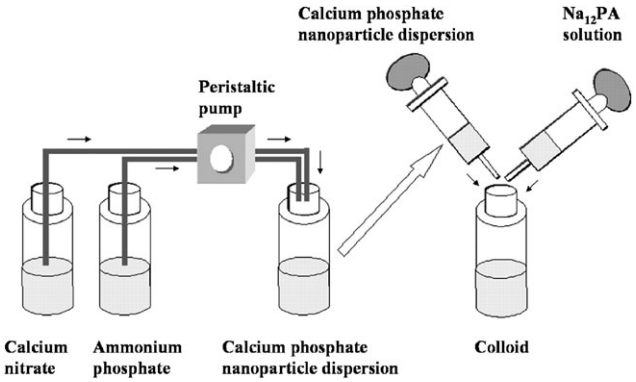

Fig. 2 Schematic diagram of the preparation of calcium phytate nanoparticles; $Na_{12}PA$ = dodecasodium phytate.

thereby to stable calcium phytate nanoparticles which may be used, *e.g.*, for scintigraphy, as a food additive or as additive to dental-care formulations.

Results and discussion

Calcium phosphate nanoparticles were prepared by rapid precipitation from aqueous solution and rapidly mixed with a solution of sodium phytate (Fig. 2). By this procedure, the immediate precipitation of calcium phytate as an insoluble salt was prevented, presumably by the adsorption of negatively charged phytate anions on the calcium phosphate surface. This led to a strongly negative charge which prevented further agglomeration. The calcium phosphate particles thereby served as a template for the precipitation of calcium phytate. The phosphate anions are subsequently exchanged by phytate anions as will be shown below. The tentative mechanism is depicted in Fig. 3.

Stable particles were only obtained in a narrow concentration range of calcium phosphate to sodium phytate (Table 1). A molar ratio of calcium to phytate between 2.5 : 1 and 1.25 : 1 gave the best results. If the ratio of calcium to phytate was higher, only agglomerated nanoparticles (which rapidly precipitated) were found, probably due to insufficient electrostatic stabilization. If it was smaller, only a very small amount of particles was found, probably due to the formation of water-soluble calcium-phytate complexes. In the optimal range, the particles had the highest negative charge; therefore we conclude that they are stabilized by electrostatic repulsion. These colloids were stable for about two weeks at room temperature before any sign of sedimentation occurred.

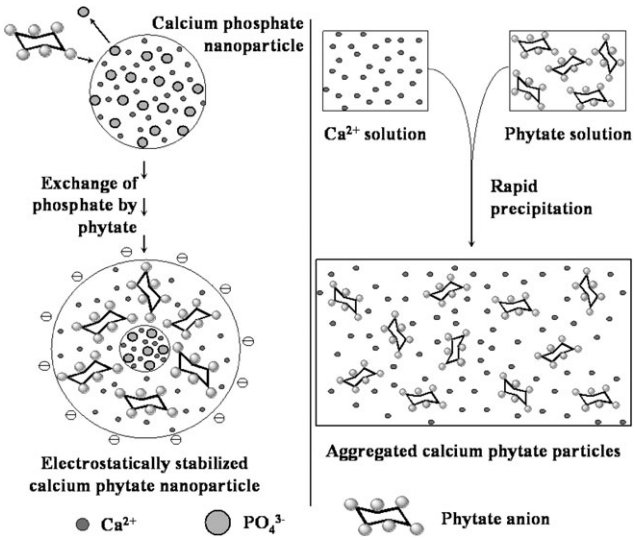

Fig. 3 Schematic view of the exchange of phosphate by phytate on the surface of nanoparticles (left), preventing the immediate precipitation of calcium phytate (right). The colloidal stabilization of the calcium phytate nanoparticles is due to their strongly negative charge.

Fig. 4 displays the dynamic light scattering data for the stable colloidal dispersions. Scanning electron microscopy showed the morphology and size of the functionalized calcium phosphate particles (Fig. 5), confirming the data from dynamic light scattering. All particles are approximately spherical and their size is very uniform under a given set of conditions. Note that all particles appear agglomerated due to the drying process that precedes the SEM experiment. Therefore, the DLS data are necessary to distinguish between dispersed and agglomerated particles while they are still in dispersion.

The IR spectrum of the calcium phytate nanoparticles showed that they consist of calcium phytate (Fig. 6). The adsorbed water molecules gave a weak absorption band around 1645 cm^{-1} and a broad absorption band around 3400 cm^{-1}. Two broad bands around 1130 and 542 cm^{-1} were assigned to PO_4^{2-} groups. The bands at 991, 903, 843 and 795 cm^{-1} were assigned to the C–O–P vibrations from the 5ax/1eq

Table 1 Properties of calcium phytate colloids from dynamic light scattering (DLS) and scanning electron microscopy (SEM). In all cases, the effective concentrations in the solution after mixing and dilution are given. The polydispersity index (PDI) was obtained from dynamic light scattering (DLS)

$[Ca^{2+}]$/mM	$[PO_4^{3-}]$/mM	[phytate]/mM	$[Ca^{2+}]$: [phytate]	Particle size from DLS/nm	PDI	Zeta potential/mV	Particle size by SEM/nm
4.5	2.7	0.03	150 : 1	>1000	—	−6(4)	Only agglomerates (precipitates)
4.5	2.7	0.3	15 : 1	>1000	—	−22(4)	were found
4.5	2.7	0.9	5 : 1	>1000	—	−43(5)	
4.5	2.7	1.8	2.5 : 1	297	0.193	−52(6)	*ca.* 250
0.75	0.45	0.3	2.5 : 1	60	0.209	−56(6)	*ca.* 30–40
4.5	2.7	3	1.5 : 1	148	0.144	−52(10)	*ca.* 100
4.5	2.7	3.6	1.25 : 1	184	0.120	−50(10)	Only very few particles were found
4.5	2.7	4.5	1 : 1	>500	—	−37(13)	
4.5	2.7	5.4	0.83 : 1	>500	—	−43(5)	

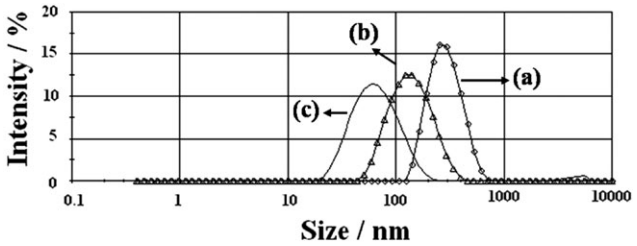

Fig. 4 Size distribution data from dynamic light scattering (DLS) of calcium phytate nanoparticles prepared with (a) $[Ca^{2+}] = 4.5$ mM and [phytate] = 1.8 mM, (b) $[Ca^{2+}] = 4.5$ mM and [phytate] = 3 mM and (c) $[Ca^{2+}] = 0.75$ mM and [phytate] = 0.3 mM.

conformation of phytate.[26] The C–O stretching vibration was observed at 1398 cm^{-1}. Compared to precipitated calcium phytate, the small shifts in the vibrational bands of functionalized particles were probably due to different calcium concentrations in the samples. We detected the characteristic vibrational bands of hydroxyapatite (1105, 1036, 602 and 563 cm^{-1}) only at a high ratio of calcium to phytate (>5 : 1), *i.e.* when agglomerates were formed (Table 1).

X-Ray powder diffraction showed that the calcium phytate nanoparticles were X-ray amorphous similarly to the precipitated calcium phytate (Fig. 7). Unfortunately, no literature data exist for crystalline calcium phytate; only X-ray amorphous phases were reported. Only for agglomerated samples with a high calcium to phytate ratio (>5 : 1) we observed (broad) diffraction peaks of hydroxyapatite (data not shown).

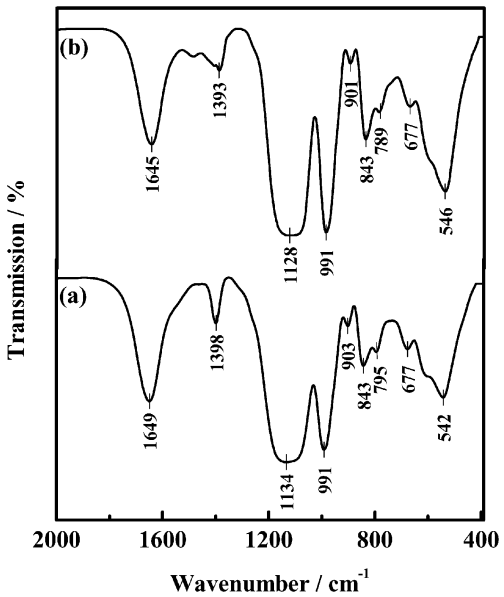

Fig. 6 IR spectra of calcium phytate nanoparticles prepared with $[Ca^{2+}] = 4.5$ mM and [phytate] = 3 mM, obtained by filtration (a), and of precipitated calcium phytate (b).

By elemental analysis, it was confirmed that the particles consisted of hexacalcium phytate plus some adhering water (about 21 wt%), except for high ratios of calcium to phytate where calcium phosphate was still present (Table 2). In these cases, the exchange of phosphate by phytate was not

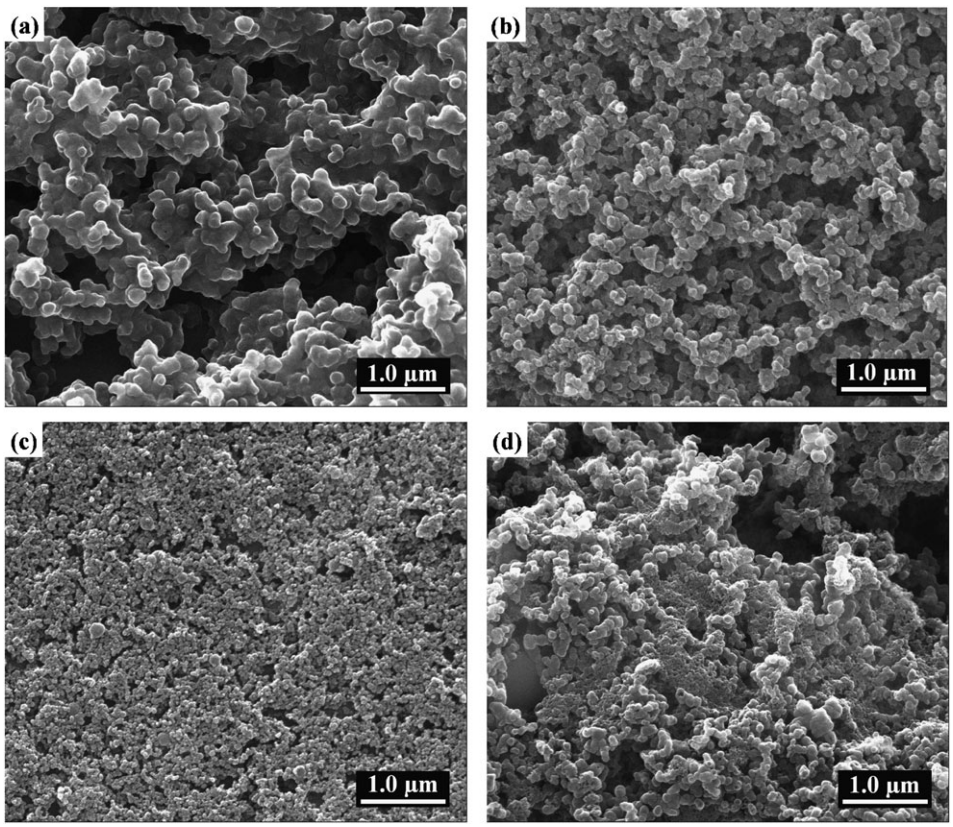

Fig. 5 SEM pictures of calcium phytate nanoparticles prepared with (a) $[Ca^{2+}] = 4.5$ mM and [phytate] = 1.8 mM, (b) $[Ca^{2+}] = 4.5$ mM and [phytate] = 3 mM, (c) $[Ca^{2+}] = 0.75$ mM and [phytate] = 0.3 mM, and (d) $[Ca^{2+}] = 4.5$ mM and [phytate] = 0.9 mM (agglomerated sample).

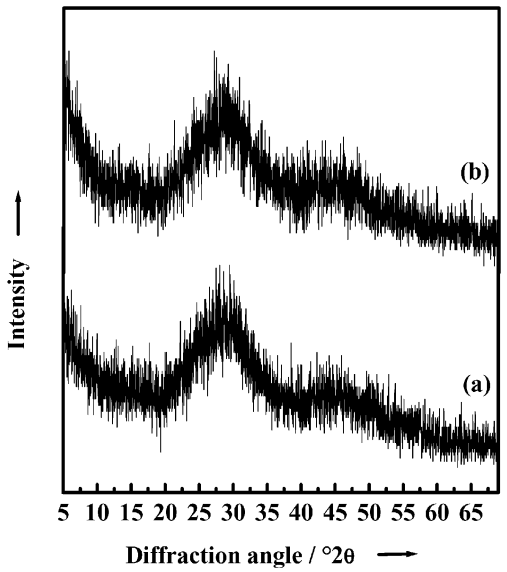

Fig. 7 X-Ray powder diffractograms of calcium phytate nanoparticles prepared with $[Ca^{2+}] = 4.5$ mM and [phytate] = 3 mM, obtained by filtration (a), and of precipitated calcium phytate (b). The samples were almost fully amorphous.

quantitative. Our attempts to determine the content of phosphate as molybdate complex gave no satisfactory results, probably because the organic phosphate in the phytate was only partly susceptible to this reaction. The data from elemental analysis were qualitatively confirmed by energy-dispersive X-ray spectrometry in the SEM.

Conclusions

The direct synthesis of calcium phytate by mixing a calcium salt and a phytate salt does not lead to a stable colloid, probably due to aggregation and crystal growth. If calcium phosphate nanoparticles are used as nuclei, the phosphate anion is exchanged by phytate and a stable colloid of calcium phytate is obtained. However, the ratio of calcium to phytate must be in a narrow range around 1.5 : 1 to obtain a stable colloid. If calcium phosphate is present in excess, the particles still contain calcium phosphate and precipitation occurs. If phytate is present in excess, dissolution of the particles occurs, probably by complexation of calcium ions by phytate ions. These colloids have the major advantage to consist of a biologically compatible material with no stabilizers being necessary. They are stable for about two weeks before agglomeration occurs.

Experimental

Preparation of calcium phytate nanoparticles

Calcium phosphate nanoparticles were prepared by rapidly pumping aqueous solutions of $Ca(NO_3)_2{\cdot}4H_2O$ (3 mM and 18 mM, pH 9) and $(NH_4)_2HPO_4$ (1.8 and 10.8 mM, pH 9) with an equal volume rate into a stirred vessel (Fig. 2).[27] The ratio of calcium to phosphate (5 : 3) always corresponded to that in hydroxyapatite, $Ca_5(PO_4)_3(OH)$, the calcium phosphate phase which is formed under these conditions.[19] A few seconds after mixing, the dispersed calcium phosphate nanoparticles were taken up with a syringe. The colloids were then prepared by rapidly mixing an aqueous solution of dodecasodium phytate ($Na_{12}PA$) and the dispersed calcium phosphate nanoparticles in a 10 ml : 10 ml ratio. The concentration of the sodium phytate solution was varied from 0.06 to 10.8 mM. Due to this mixing and dilution process, the effective concentrations of Ca^{2+} were 0.75 and 4.5 mM, of PO_4^{3-} 0.45 and 2.7 mM, and of sodium phytate 0.03 to 5.4 mM. The final pH of the colloid was between 8 and 9. The particles were studied either as a dispersion or after collection on a membrane filter (supor®-100 by PALL Life sciences). The filtered nanoparticles were washed with 100 ml of absolute ethanol and dried in air. Ultrapure water (Purelab ultra instrument from ELGA) was used for all preparations.

Hexacalcium phytate (Ca_6PA) was prepared by pumping aqueous solutions of $Ca(NO_3)_2{\cdot}4H_2O$ (18 mM, pH = 9.5) and sodium phytate (3 mM, pH = 10.5) into a stirred vessel which led to immediate precipitation. After 30 min stirring the precipitate was collected by filtration. The powder was washed with ethanol and dried in air at 37 °C.

Characterization techniques

The products were characterized by X-ray powder diffraction (XRD; STOE IP-PSD diffractometer; Cu-Kα radiation, λ = 1.54 Å), infrared spectroscopy (FTIR; Bruker-Vortex 70 instrument), and scanning electron microscopy coupled with energy-dispersive X-ray spectroscopy (SEM-EDX; ESEM Quanta 400 FEG, FEI; gold–palladium [80 : 20]-sputtered samples; EDX detector: S-UTW-Si(Li)). Dynamic light scattering and zeta potential determinations were performed with a Zetasizer nanoseries (Malvern Nano-ZS, laser: λ = 532 nm) instrument. The dodecasodium salt of phytic acid ($Na_{12}PA$) was purchased from Aldrich and used as received.

Table 2 Elemental analysis data of calcium phosphate/calcium phytate colloids, obtained by filtration and drying in air at 37 °C; CaP = calcium phosphate

$[Ca^{2+}]$/mM	$[PO_4^{3-}]$/mM	[phytate]/mM	C (wt%)	H (wt%)	Ca (wt%)	Overall composition
4.5	2.7	0.05	0.84	1.16	33.55	CaP + Ca_6PA + H_2O
4.5	2.7	0.5	2.55	1.93	29.38	CaP + Ca_6PA + H_2O
4.5	2.7	1.5	6.10	2.81	19.75	Ca_6PA + H_2O
4.5	2.7	3	7.13	2.89	21.08	Ca_6PA + H_2O
0.75	0.45	0.3	6.74	2.65	21.39	Ca_6PA + H_2O
Precipitated calcium phytate			6.43	3.45	21.26	Ca_6PA + H_2O
Computed for $Ca_6PA{\cdot}13.1H_2O$			6.41	2.89	21.39	
Computed for calcium phytate (Ca_6PA)			8.11	0.68	27.07	

References

1. B. F. Harland and E. R. Morris, *Nutr. Res.*, 1995, **15**, 733.
2. V. Raboy, *Phytochemistry*, 2003, **64**, 1033.
3. F. J. McClure, *J. Dent. Res.*, 1963, **42**, 693.
4. F. J. McClure, *Science*, 1964, **144**, 1337.
5. G. N. Jenkins, in *The Refinement of Foods in Relation to Dental Caries*, ed. P. H. Staples, Academic Press, New York, 1966.
6. H. Nordbö and G. Rölla, *J. Dent. Res.*, 1972, **51**, 800.
7. R. Greiner, U. Konietzny and K. D. Jany, *J. Ernaehrungsmed.*, 2006, **8**(3), 18.
8. A. Wise, *Bull. Environ. Contam. Toxicol.*, 1981, **27**, 630.
9. A. Wise, *Bull. Environ. Contam. Toxicol.*, 1982, **29**, 550.
10. L. R. Isbrandt and R. P. Oertel, *J. Am. Chem. Soc.*, 1980, **102**, 3144.
11. L. G. Barrientos and P. P. N. Murthy, *Carbohydr. Res.*, 1996, **296**, 39.
12. J. Emsley and S. Niazi, *Phosphorus Sulfur Relat. Elem.*, 1981, **10**, 401.
13. C. Brigando, J. C. Mossoyan, F. Favier and D. Benlian, *J. Chem. Soc., Dalton Trans.*, 1995, 575.
14. S. K. Imam and M. Killingsworth, *World J. Nucl. Med.*, 2005, **4**, 179.
15. H. Higashi, S. Natsugoe, Y. Uenosono, K. Ehi, T. Arigami, Y. Nakabeppu, M. Nakajo and T. Aikou, *J. Surg. Res.*, 2004, **121**, 1.
16. J. Campbell, J. C. Bellen, R. J. Baker and D. J. Cook, *J. Nucl. Med.*, 1981, **22**, 157.
17. M. A. A. Al-Janabi, *J. Labelled Compd. Radiopharm.*, 1989, **27**, 1137.
18. S. Weiner and H. D. Wagner, *Annu. Rev. Mater. Sci.*, 1998, **28**, 271.
19. S. V. Dorozhkin and M. Epple, *Angew. Chem., Int. Ed.*, 2002, **41**, 3130.
20. A. Heiss, A. DuChesne, B. Denecke, J. Grötzinger, K. Yamamoto, T. Renné and W. Jahnen-Dechent, *J. Biol. Chem.*, 2003, **278**, 13333.
21. R. Westenfeld, W. Jahnen-Dechent and M. Ketteler, *Trends Cardiovasc. Med.*, 2007, **17**, 124.
22. A. Lebugle, F. Pellé, C. Charvillat, I. Rousselot and J. Y. Chane-Ching, *Chem. Commun.*, 2006, 606.
23. V. Sokolova, O. Prymak, W. Meyer-Zaika, H. Cölfen, H. Rehage, A. Shukla and M. Epple, *Mat.-wiss. u. Werkstofftech.*, 2006, **37**, 441.
24. V. Sokolova and M. Epple, *Angew. Chem., Int. Ed.*, 2008, **47**, 1382.
25. A. W. Xu, Q. Yu, W. F. Dong, M. Antonietti and H. Coelfen, *Adv. Mater.*, 2005, **17**, 2217.
26. Z. He, C. W. Honeycutt, T. Zhang and P. M. Bertsch, *J. Environ. Qual.*, 2006, **35**, 1319.
27. T. Welzel, W. Meyer-Zaika and M. Epple, *Chem. Commun.*, 2004, 1204.

